Title

The Listeria monocytogenes Hibernation-Promoting Factor Is Required for the Formation of 100S Ribosomes, Optimal Fitness, and Pathogenesis

Journal

Journal of Bacteriology, 197(3)

ISSN

0021-9193

Authors

Kline, Benjamin C

McKay, Susannah L

Tang, William W

et al.

Publication Date

2015-02-01

DOI

10.1128/jb.02223-14

Peer reviewed

JB
Journals.ASM.org

The *Listeria monocytogenes* Hibernation-Promoting Factor Is Required for the Formation of 100S Ribosomes, Optimal Fitness, and Pathogenesis

Benjamin C. Kline,[a]* Susannah L. McKay,[a] William W. Tang,[a] Daniel A. Portnoy[a,b]

Department of Molecular and Cell Biology[a] and School of Public Health,[b] University of California, Berkeley, California, USA

During exposure to certain stresses, bacteria dimerize pairs of 70S ribosomes into translationally silent 100S particles in a process called ribosome hibernation. Although the biological roles of ribosome hibernation are not completely understood, this process appears to represent a conserved and adaptive response that contributes to optimal survival during stress and post-exponential-phase growth. Hibernating ribosomes are formed by the activity of one or more highly conserved proteins; gammaproteobacteria produce two relevant proteins, ribosome modulation factor (RMF) and hibernation promoting factor (HPF), while most Gram-positive bacteria produce a single, longer HPF protein. Here, we report the formation of 100S ribosomes by an HPF homolog in *Listeria monocytogenes*. *L. monocytogenes* 100S ribosomes were observed by sucrose density gradient centrifugation of bacterial extracts during mid-logarithmic phase, peaked at the transition to stationary phase, and persisted at lower levels during post-exponential-phase growth. 100S ribosomes were undetectable in bacteria carrying an *hpf*::*Himar1* transposon insertion, indicating that HPF is required for ribosome hibernation in *L. monocytogenes*. Additionally, epitope-tagged HPF cosedimented with 100S ribosomes, supporting its previously described direct role in 100S formation. We examined *hpf* mRNA by quantitative PCR (qPCR) and identified several conditions that upregulated its expression, including carbon starvation, heat shock, and exposure to high concentrations of salt or ethanol. Survival of HPF-deficient bacteria was impaired under certain conditions both *in vitro* and during animal infection, providing evidence for the biological relevance of 100S ribosome formation.

Listeria monocytogenes is a Gram-positive, food-borne, facultative intracellular pathogen that infects a broad range of vertebrate hosts (1, 2). The bacterium leads a saprophytic lifestyle in the environment and is commonly found in soil, water, and decaying organic matter. *L. monocytogenes* most commonly causes disease in elderly, immunocompromised, or pregnant individuals but can pose a general public health risk in cases of severe food contamination. Because of its ability to shift quickly between saprophytic growth in the environment and potentially lethal pathogenesis upon contacting a host, *L. monocytogenes* has been referred to as a bacterial "Dr. Jekyll and Mr. Hyde" (3). The ability to tolerate or thrive in a variety of unfavorable conditions, including high salt, low pH, and refrigeration temperatures, has made *L. monocytogenes* a formidable challenge to the food industry (1, 2). Therefore, it is important to understand the set of factors that enable *L. monocytogenes* to survive so effectively in a wide variety of inhospitable environments. Some of these factors are involved in conserved bacterial stress responses, while others may be specific to *Listeria* spp. and their close relatives (4).

Ribosome hibernation is thought to be an alternative to the classical ribosome recycling pathway, shunting ribosomes into mRNA- and tRNA-free 70S complex dimers that sediment at 100S (5). These complexes appear to be translationally inactive *in vitro* but can dissociate within minutes to release translationally competent ribosomes (6, 7). The relative abundance of 100S ribosomes varies dramatically over the course of growth in broth, and this temporal profile of hibernation varies from one bacterial species to another. In *Escherichia coli*, 100S ribosomes are barely detectable in lysates from rapidly growing bacteria but increase dramatically in abundance upon entry to stationary phase, substantially outnumbering 70S ribosomes in stationary-phase lysates (8). In contrast, 100S ribosomes are abundant in log-phase lysates of the Gram-positive bacterium *Staphylococcus aureus*, increasing to a peak upon entry to stationary phase and decreasing gradually in quantity over the next several hours of post-exponential-phase growth (discussed further below) (9). Given their presumed role in downregulating translation, the function of 100S ribosomes during logarithmic-phase growth in *S. aureus* remains unclear.

The genes that enable 100S ribosome formation are present in most bacteria, but the distribution of these genes varies in Gram-positive and -negative species (10). *E. coli* and other gammaproteobacteria perform ribosome hibernation through the combined activities of ribosome modulation factor (RMF) and a "short" hibernation promoting factor (HPF), while Gram-positive bacteria do not possess RMF and instead produce a single "long" HPF (11, 12). The short and long forms of HPF produce distinct types

Received 31 August 2014 **Accepted** 15 November 2014

Accepted manuscript posted online 24 November 2014

Citation Kline BC, McKay SL, Tang WW, Portnoy DA. 2015. The *Listeria monocytogenes* hibernation-promoting factor is required for the formation of 100S ribosomes, optimal fitness, and pathogenesis. J Bacteriol 197:581–591. doi:10.1128/JB.02223-14.

Editor: V. J. DiRita

Address correspondence to Daniel A. Portnoy, portnoy@berkeley.edu.

* Present address: Benjamin C. Kline, Emerald Therapeutics, South San Francisco, California, USA.

doi:10.1128/JB.02223-14

of 100S ribosomes with different stabilities and temporal profiles (13). The long HPF bears a C-terminal extension that has been shown in *Lactococcus lactis* to contribute to ribosome dimerization in the same structural manner as RMF does in Gram-negative bacteria (14).

Because ribosome hibernation is induced during entry to stationary phase where nutrients are low and growth is slow, it has been suggested that 100S ribosomes downregulate global translation and store ribosomes for future use (15). However, the functions of ribosome hibernation appear to be diverse and have not yet been fully explored. Although ribosome hibernation in *S. aureus* is dependent on the nutrient content of the growth medium, 100S ribosomes are present in *S. aureus* extracts at all phases of growth (9). A recent report on hibernation in *Bacillus subtilis* established the importance of a long HPF homolog in 100S ribosome formation during amino acid starvation but did not discuss the functional importance of 100S ribosomes (16). The physiological consequences of hibernation in bacteria expressing long HPF have only recently begun to be elucidated, with the demonstration that *L. lactis* lacking HPF exhibits defects surviving and recovering from prolonged starvation (14). Transcription and/or translation of both *rmf* and *hpf* are upregulated at the entry to stationary phase (12, 17). Accordingly, RMF-deficient *E. coli* displays a substantial survival defect during prolonged post-exponential-phase growth (7). A report examining gene regulation and stress tolerance in *Pseudomonas aeruginosa* biofilms showed that RMF is preferentially expressed by bacteria deep in biofilms and may contribute to survival (18). Hibernation-associated factors also appear to be important for optimal survival of various stresses in stationary phase, including acid, osmotic, and heat stress, although how 100S ribosomes contribute to survival is uncertain (19–21).

In addition to *L. monocytogenes* and *S. aureus*, several other important human pathogens, including *Mycobacterium tuberculosis*, *Bacillus anthracis*, and the *Clostridium* species contain homologs of long HPF but none of RMF (10). Since RMF-dependent hibernation is important in the Gram-negative bacterial response to a variety of stresses and enhances survival under adverse conditions, it is important to determine whether long-HPF-dependent hibernation serves equally critical roles. In this work, we examined ribosome hibernation in *L. monocytogenes*. We determined that *L. monocytogenes* forms 100S ribosomes in a temporal pattern similar to *S. aureus*; 100S ribosomes were detectable at nearly every point in broth growth, peaking at the entry to stationary phase and then decreasing to a lower, steady level for several hours. HPF expression was regulated in patterns similar to those seen in RMF/short-HPF-producing bacteria and was responsive to growth phase, stress, and nutrient deprivation. We showed that HPF was indispensable for ribosome hibernation in *L. monocytogenes* and that it comigrated through sucrose gradients predominantly with 100S ribosomes. Although no survival defect was apparent in post-exponential-phase monoculture, HPF-deficient *L. monocytogenes* showed a substantial competitive disadvantage in post-exponential-phase coculture with wild-type (WT) *L. monocytogenes*. Finally, mouse infection by both the intravenous and oral routes also showed a marked defect for *hpf*-deficient bacteria. Combined, these results suggest that hibernation plays an important role in *L. monocytogenes* pathogenesis and adaptation to stress.

MATERIALS AND METHODS

Bacterial strains and culture conditions. The bacterial strains used in this study are listed in Table 1. *L. monocytogenes* strains were cultured in brain heart infusion medium (BHI; Difco, Detroit, MI). *Escherichia coli* strains were cultured in Luria-Bertani medium (LB). Unless otherwise noted, bacterial cultures used for experiments were started by diluting overnight cultures to an optical density at 600 nm (OD_{600}) of 0.02. The following antibiotics were used at the concentrations specified: erythromycin (Erm), 1 μg/ml; chloramphenicol (Cm), 10 μg/ml; streptomycin (Sm), 200 μg/ml.

Conditioned medium and stress treatment experiments. Conditioned medium was generated by inoculating fresh medium with WT bacteria as described above and growing it at 37°C with shaking for the specified length of time. Bacteria were then removed by centrifugation (10 min at 1,700 × *g*) and filtration (0.22-μm-pore-size Stericup vacuum filter) and stored at 4°C until use. Conditioned-medium transcriptional regulation experiments were performed at mid-log phase (OD ≈ 0.4); bacteria were pelleted and resuspended in conditioned medium and incubated for 30 min at 37°C with shaking before flash freezing and RNA extraction. Stress treatments were also performed at mid-log phase; stress-inducing agents were added to the existing medium, and bacteria were incubated for 5 min at 37°C (or 46°C for heat stress-treated samples) with shaking before flash freezing and RNA extraction.

Preparation of crude ribosomes. Preparation and fractionation of ribosome samples were performed using a protocol adapted from Ueta et al. (9). Cowpea mosaic virus (CPMV) fragments of 68, 95, and 115S were used as sedimentation standards. All buffers were prepared with nuclease-free water and reagent powders. Cultures of *L. monocytogenes* (100 ml) in BHI were inoculated to an OD_{600} of 0.02 to 0.04 in 500-ml Erlenmeyer flasks and grown at 37°C with shaking until the desired growth phase was reached. Bacteria were harvested by pelleting 10 min at 3,000 × *g* in a tabletop centrifuge and then resuspended in 1.2 ml ribosome extraction (RE) buffer (20 mM Tris-HCl [pH 7.6], 15 mM magnesium acetate, 100 mM ammonium acetate, 6 mM 2-mercaptoethanol, 2 mM phenylmethanesulfonyl fluoride [PMSF]) per 100 ml of culture. Cell suspensions were transferred to 1.5-ml microcentrifuge tubes along with ≈250 μl of sterile 0.1-mm zirconia/silica beads (BioSpec, Bartlesville, OK), and bacterial cells were disrupted by vortexing for 10 min at 4°C. Bacterial lysates were separated from beads, and cell debris was pelleted in a microcentrifuge for 15 min at 9,000 × *g* at 4°C. Supernatants were transferred to separate tubes on ice; pellets were resuspended in 600 μl fresh RE buffer and pelleted again for 15 min at 9,000 × *g* at 4°C. Supernatants were combined and layered onto 3-ml pads of 30% sucrose in ribosome fractionation (RF) buffer (20 mM Tris-HCl [pH 7.6], 15 mM magnesium acetate, 100 mM ammonium acetate, 6 mM 2-mercaptoethanol) in 10.4-ml polycarbonate bottles (Beckmann Coulter, Brea, CA). Bottles were very gently filled to the shoulder with RF buffer using a Pipet-Aid and centrifuged in a type 70.1 Ti rotor (Beckman) in a Beckman XL-70 preparative ultracentrifuge for 2 h at 65,000 rpm (290,000 × *g*) at 4°C. Supernatants were gently decanted, and then pellets were washed with 1 ml RF buffer each and resuspended in 500 μl RF buffer each using a glass pipette. Resuspended crude ribosome (CR) samples were transferred to 1.5-ml microcentrifuge tubes and stored at −20°C until separation on sucrose gradients.

Sucrose density gradient centrifugation. Sucrose gradients (11 ml, 5 to 21%) in RF buffer were prepared by progressively layering 21, 17, 13, 9, and 5% sucrose-RF buffer solutions on top of one another in 2.2-ml increments in 12-ml open-top clear ultracentrifuge tubes (Denville Scientific, Metuchen, NJ). Gradients were agitated by gently plunging a sealed glass pipette into each twice and then sealed with Parafilm and allowed to equilibrate for 24 to 48 h at 4°C. CR samples were thawed on ice, and nucleic acid content was measured by A_{260}. A total of 150 μg of each sample was diluted to a 500-μl total volume in RF buffer and layered gently onto an equilibrated 5%-to-21% gradient. Gradients were centrifuged in an SW41 Ti rotor (Beckman) for 2 h at 37,000 rpm (170,000 × *g*)

TABLE 1 Plasmids, strains, and primers used in this study

Plasmid, strain, or primer	Description	Reference, source, or sequence[c]
Plasmids		
pBHE261	*L. monocytogenes* deletion suicide vector	25[a]
pPL2	*L. monocytogenes* integration vector	28
pBK23	pPL2-*hpf*	This study
pBK27	pPL2-*hpf*-CHis	This study
pBK31	pPL2-*hpf*-CFLAG	This study
pTB69	pBHE261-Δ*hpf*	This study
Strains		
10403S	Wild-type reference strain	48
DP-L3903	Erm^r control strain	49
BK-L33	Transposon insertion in *hpf*	This study[b]
BK-L34	BK-L33 carrying $HPF_{6\times His}$	This study
BK-L44	BK-L33 carrying HPF_{FLAG}	This study
SM-69	Δ*hpf*	This study
Primers		
BK-124	*hpf* qPCR forward	GAAGTAACAGAACCGATTCGAGA
BK-125	*hpf* qPCR reverse	CTCCACTTGTTTCTTCTGCAC
JZ-199	*bglA* qPCR forward	ATAAGTTGGCATTGCTAGGAC
JZ-200	*bglA* qPCR reverse	ACCTATACCAAGCTGTCCAC
BK-150	*mreB* qPCR forward	TTGATTTAGGGACAGCGAACAC
BK-151	*mreb* qPCR reverse	CTACCAATCATATTTTTAGCATCGC
TB-36	*hpf* deletion 5′ forward	atatggatccAAGCTATCTCTCACATTCAAAAAATGAATCAA
TB-37	*hpf* deletion 5′ reverse	TAAATTATTATTTTAAATTAGTTTGTTTCACGAATGTTGTACTTAAGCATAGCAATT
TB-38	*hpf* deletion 3′ forward	AATTGCTATGCTTAAGTACAACATTCGTGAAACAAACTAATTTAAAATAATAATTTA
TB-39	*hpf* deleteion 3′ reverse	attagtcgacATATAGAATAGTCGATTTTTCCGCTTCTCCA
BK-110	*hpf* promoter and SalI site	attagtcgacTATATACACCACAGGAAGCACACTT
BK-119	*hpf* 3′ and 6×His and EagI site	taatcggccgTTAgtggtggtggtggtggtgGTTTGTTTCAATCAAACCATACTTACC
BK-140	*hpf* 3′ and FLAG and EagI site	aatcggccgTTActtgtcatcgtcatccttgtaatcGTTTGTTTCAATCAAACCATACTT

[a] Derivative of pKSV7 (50).
[b] Thanks to Jess Leber.
[c] Capital letters indicate genome-complementary regions; lowercase letters indicate noncomplementary engineered regions (restriction sites, tags, and overhangs); underlining indicates restriction sites.

and at 4°C in a Beckman XL70 preparative ultracentrifuge. Gradients were analyzed and fractions collected using an ISCO gradient fractionator.

Quantitative Western blotting. Quantitative Western blot analyses were performed using a LiCor Odyssey scanner (LiCor, Lincoln, NE). Blocking was performed with Odyssey blocking buffer (LiCor) mixed 1:1 with phosphate-buffered saline (PBS; Gibco). Primary staining was performed using either the anti-FLAG M2 antibody (Sigma-Aldrich, St. Louis, MO) at a 1:1,000 dilution or the His-probe (G18) antibody (Santa Cruz Biotechnology, Santa Cruz, CA) at a 1:500 dilution. Secondary staining was performed using IRDye 680 polyclonal goat anti-mouse antibody (LiCor). Blots were analyzed using the LiCor Odyssey scanner.

Competition assays in broth. Two *L. monocytogenes* strains to be competed with one another were grown separately overnight at 37°C with shaking and then added to 50 ml BHI in a 250-ml Erlenmeyer flask to a final OD_{600} of 0.02 in a 1:1 ratio (as calculated by OD_{600}). OD measurement and plating for CFU were performed immediately and then once every 24 h thereafter for a period of 5 to 8 days. At each time point, each competitive culture was serially diluted and spread onto plates containing LB or LB and 1 μg/ml erythromycin. The ratio of Erm^r CFU/(total CFU − Erm^r CFU) was interpreted as the ratio of transposon-carrying bacteria to WT bacteria. Randomly selected colonies were patched from LB plates to plates containing LB and 1 μg/ml Erm to verify that the above calculation faithfully reflected the number of Erm^r CFU in the culture.

Quantitative RT-PCR. Bacterial RNA was isolated as previously described (22). Contaminating DNA was removed using the Turbo DNA*free* kit (Ambion/Life, Carlsbad, CA). Reverse transcription (RT) was performed using iScript reverse transcriptase (Bio-Rad, Hercules, CA), and quantitative PCR (qPCR) was performed using SYBR FAST qPCR master mix (KAPA Biosystems, Cambridge, MA). Primers (all listed 5′ to 3′) against *hpf* (GAAGTAACAGAACCGATTCGAGA and CTCCACTTGTTTCTTCTGCAC), *bglA* (ATAAGTTGGCATTGCTAGGAC and ACCTATACCAAGCTGTCCAC), and *mreB* (TTGATTTAGGGACAGCGAACAC and CTACCAATCATATTTTTAGCATCGC) were used to detect experimental (*hpf*) and control (*bglA* and *mreB*) transcripts. Amplification and detection were performed in an Mx3000P thermal cycler, and data were analyzed using the MxPro software (Stratagene, La Jolla, CA). qPCRs were each performed with multiple reference genes, and while the trends were always similar, the data presented were in reference to genes with the least variation under those experimental conditions.

Generation of in-frame deletion mutants. In-frame deletions were generated as previously described (23). Briefly, ~900-bp fragments upstream and downstream of the *hpf* open reading frame (ORF), including the first seven and the last four codons of the gene, were amplified with the primer pairs AAGCTATCTCTCACATTCAAAAAATGAATCAA/taaattattattttaaattagtttgtttcACGAATGTTGTACTTAAGCATAGCAATT and AATTGCTATGCTTAAGTACAACATTCGTgaaacaaactaatttaaaataataattta/tggagaagcggaaaaatcgactattctatat. Upstream and downstream fragments were joined by splicing by overhang extension PCR (SOE PCR) (24), cloned into the *oriT*-containing suicide vector pBHE261 (25), and transferred into *L. monocytogenes* by conjugation. Integration and excision of the plasmid to generate an in-frame deletion were performed as previously described.

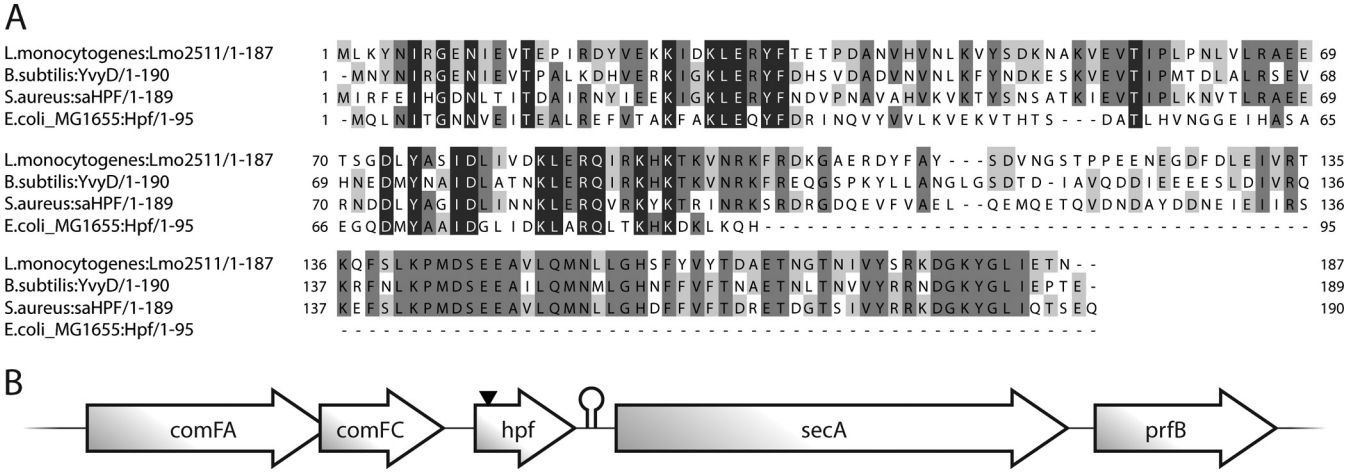

FIG 1 *L. monocytogenes* produces a long HPF homolog. (A) Alignment of *L. monocytogenes* HPF with long homologs from *S. aureus* and *B. subtilis* and a short homolog from *E. coli*, produced using ClustalW2 (43, 44) and Jalview 2 (45). Five of the six residues predicted to be important for ribosome binding in YfiA (11, 46) are conserved in *L. monocytogenes* HPF. (B) Genomic context of *L. monocytogenes hpf*. A transcriptional terminator is located 3′ of the *hpf* coding sequence. *hpf*::*Himar1* transposon position is marked by an arrowhead.

Mouse infections. All mouse infections were performed on 6- to 8-week-old female BALB/c mice (Jackson Laboratory, Bar Harbor, ME). Inocula were derived from 24-hour stationary-phase cultures grown in phosphate-buffered BHI. Doses of 3×10^4 CFU (1× the 50% lethal dose [LD_{50}]) and 1×10^8 CFU were used for intravenous and oral infections, respectively. For intravenous infections, 200 μl of bacterial suspension in PBS (Gibco) was administered by injection into the tail vein. Oral infections were carried out as previously described (26). Briefly, bacteria were suspended in melted butter and applied to 0.5-cm cubes of white bread. Food was withheld for 12 h prior to each mouse being fed a single cube of *L. monocytogenes*-inoculated bread. Both oral and intravenous infections were allowed to proceed for 48 h, and then animals were sacrificed and organs were homogenized and spread on plates to measure CFU. CFU per organ in mice infected with WT bacteria were compared directly to CFU per organ in mice infected with Δ*hpf* bacteria.

RESULTS

Identification of *lmo2511* as an *L. monocytogenes* homolog of HPF. Based on protein sequence homology, *lmo2511* is predicted to encode a long HPF homolog (referred to here as HPF) highly similar to *S. aureus* HPF (Fig. 1A). In keeping with the organization of other HPF genes of the same family, *L. monocytogenes* HPF consists of an N-terminal RaiA domain (bearing 37% identity to the *E. coli* HPF and 57% identity to the *S. aureus* HFP) and a C-terminal extension with homology only to other long HPF genes. Homologs of the *L. monocytogenes* HPF are present in each of the other known species of *Listeria*, and all are very highly similar to the *L. monocytogenes* HPF (≥88% protein sequence identity). A predicted transcriptional terminator is located just downstream of the *lmo2511* coding sequence (Fig. 1B), and tiling microarray analysis has previously shown that *lmo2511* is likely to be transcribed as a one-gene operon (27). To study the production and function of 100S ribosomes in *L. monocytogenes*, we made use of a *Himar1* transposon insertion and an in-frame deletion in the *hpf* coding sequence (*hpf*::*Himar1* and Δ*hpf*, respectively). The *hpf*::*Himar1* transposon mutant is predicted to encode a truncated, approximately 30-amino-acid fragment of the HPF protein, while the Δ*hpf* mutant retains the first seven and last three amino acids of the HPF protein but lacks the intervening 177 (Fig. 1B). The *hpf*::*Himar1* strain was used for the majority of the work below, but the two strains behaved similarly in every assay.

***L. monocytogenes* produces 100S ribosomes in an HPF-dependent manner.** To determine whether *L. monocytogenes* produces 100S ribosomes, the ribosome profile of WT *L. monocytogenes* was examined by sucrose density gradient centrifugation (SDGC). As in *S. aureus* (9), a 260-nm absorbance peak was observed that migrated through sucrose density gradients at the rate expected for a 100S complex. To examine the abundance of the 100S ribosome species at different bacterial growth phases, we analyzed ribosome samples isolated during a time course from *L. monocytogenes* grown in rich medium (Fig. 2). In these samples, 100S ribosomes were barely detectable during early-exponential-phase growth but increased in relative abundance during mid- to late-exponential phase. The abundance of 100S relative to 70S ribosomes peaked at the transition from logarithmic- to stationary-phase growth (OD_{600} of approximately 2.5 to 3.0). Upon entry into stationary phase, relative abundance of 100S dimers returned to approximately mid-log levels and was maintained at this ratio for several hours. The majority of ribosomes prepared from bacteria exposed to prolonged post-exponential-phase growth (72 to 96 h) migrated with roughly 30S mobility, an observation that might reflect ribosome degradation (8).

Bacterial extracts of *hpf* mutants were analyzed by SDGC to determine whether disruption of *hpf* influenced formation of 100S ribosomes in *L. monocytogenes*. In stark contrast to WT *L. monocytogenes*, 100S complexes were absent from ribosome samples isolated from *hpf*::*Himar1* and Δ*hpf L. monocytogenes* strains (Fig. 3A and B and data not shown). To determine whether the absence of 100S ribosomes was attributable to disruption of *hpf*, we complemented the *hpf*::*Himar1* strain using a site-specific integration vector (28) harboring the *hpf* gene and native promoter with or without a C-terminal 6×His tag. Ribosome profiles from the tagged complemented strain recovered a substantial amount of 100S dimer production (Fig. 3C). It is not clear why the 100S ribosome population was not fully restored in the complemented strain; however, it was not due to the epitope tag, since an untagged

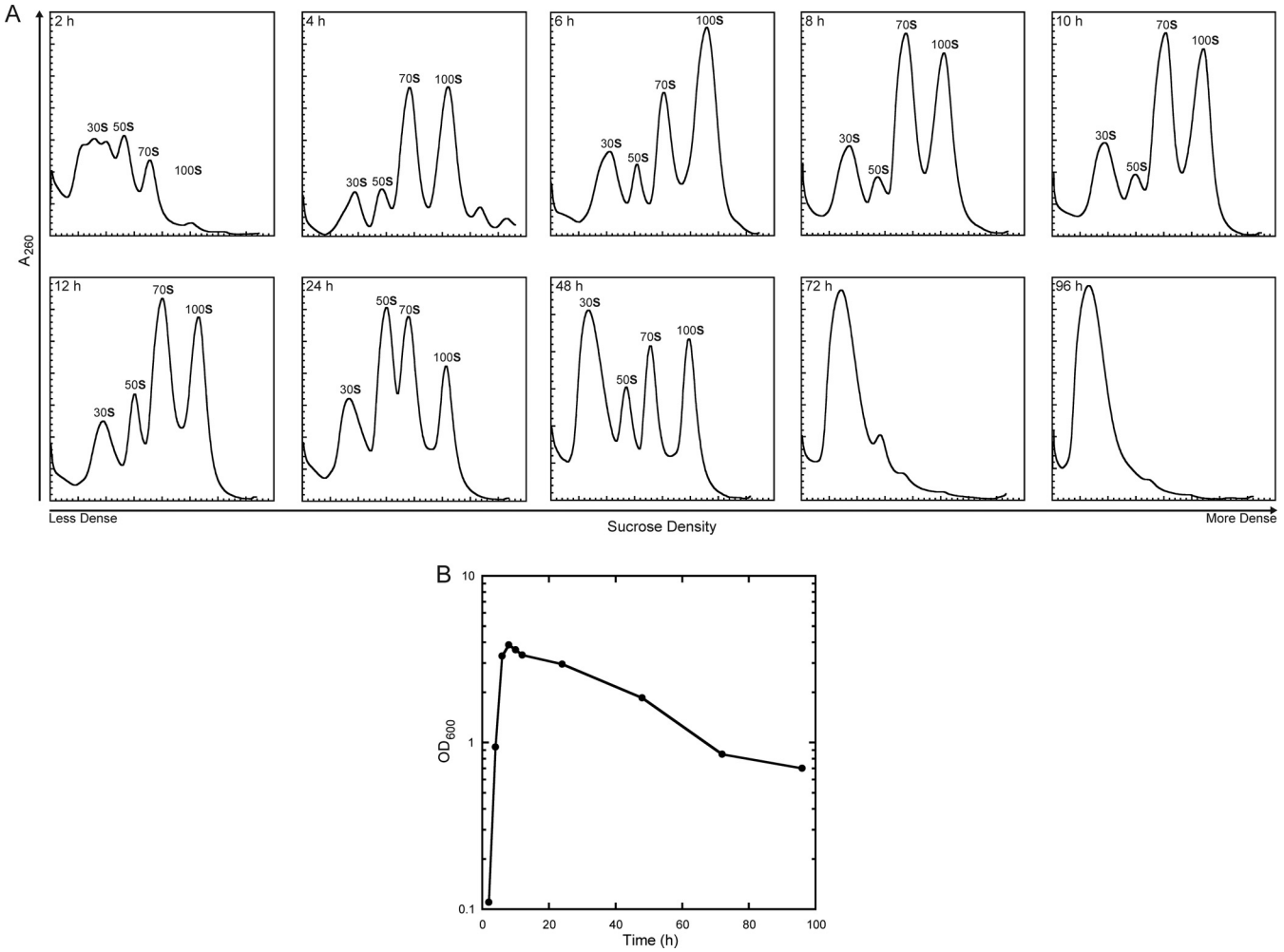

FIG 2 Time course of ribosome hibernation in *L. monocytogenes*. (A) Presence or absence of 100S ribosome dimers in *L. monocytogenes* extracts was visualized over 96 h of growth in broth by sucrose density gradient centrifugation (SDGC). Each gradient was loaded with 150 μg of total nucleic acid, as measured by A_{260} (*y* axis). Each graph depicts the fractions collected from the top (least dense) to the bottom (most dense) of the gradient on the *x* axis. The large peak at 72 and 96 h runs with the mobility of 30S particles but likely represents degraded ribosomes (8). (B) Growth curve of *L. monocytogenes* cultured in BHI at 37°C from which ribosome samples were isolated.

hpf-complemented strain produced ribosome profiles identical to those of the tagged complement (data not shown).

The *S. aureus* HPF homolog has previously been shown to associate primarily with 100S ribosome complexes during logarithmic-phase growth (9). Using the tagged $HPF_{6\times His}$ described above, we confirmed that the same occurs in *L. monocytogenes* whole-cell ribosome extracts as well. Quantitative Western blot analysis of ribosome fractions collected from late-exponential-phase *L. monocytogenes* carrying the epitope-tagged *hpf* gene showed that $HPF_{6\times His}$ comigrated through sucrose gradients predominantly with 100S dimers. Over 80% of total $HPF_{6\times His}$ was localized to fractions in which 100S complexes were the dominant species (Fig. 3D). The small amount of HPF associated with other fractions was consistent with earlier findings, as *S. aureus* HPF was previously shown to associate with 70S ribosomes in small amounts during logarithmic-phase growth and larger amounts during stationary phase (9). To confirm that the 6×His tag itself was not causing HPF localization to 100S ribosomes, a FLAG epitope tag was substituted. The resulting HPF protein showed the same pattern of localization (data not shown).

***L. monocytogenes hpf* expression is stimulated by starvation and stress.** Previous work has demonstrated that nutrient depletion induces expression of hibernation machinery (10, 16, 29). However, these modes of hibernation regulation remain unexplored in *L. monocytogenes*, and signals independent of nutrient depletion may also influence *hpf* expression and modulate ribosome hibernation. To determine what components of the growth medium influenced *hpf* expression at various points in growth, we monitored *hpf* mRNA abundance in mid-log-phase bacteria in response to conditioned medium. Conditioned media were generated by culturing WT *L. monocytogenes* in broth to a given growth phase and then removing the bacteria by centrifugation and filtration. In keeping with the observation that 100S ribosomes appeared throughout logarithmic-phase growth and peaked upon entry into stationary phase, *hpf* transcript was most abundant (approximately 100-fold) in bacteria exposed to early-stationary-phase conditioned medium. *hpf* transcript levels were substantially lower in conditioned medium from earlier in growth than later and settled at an intermediate level in medium from prolonged stationary phase (Fig. 4A). The relative magnitude and

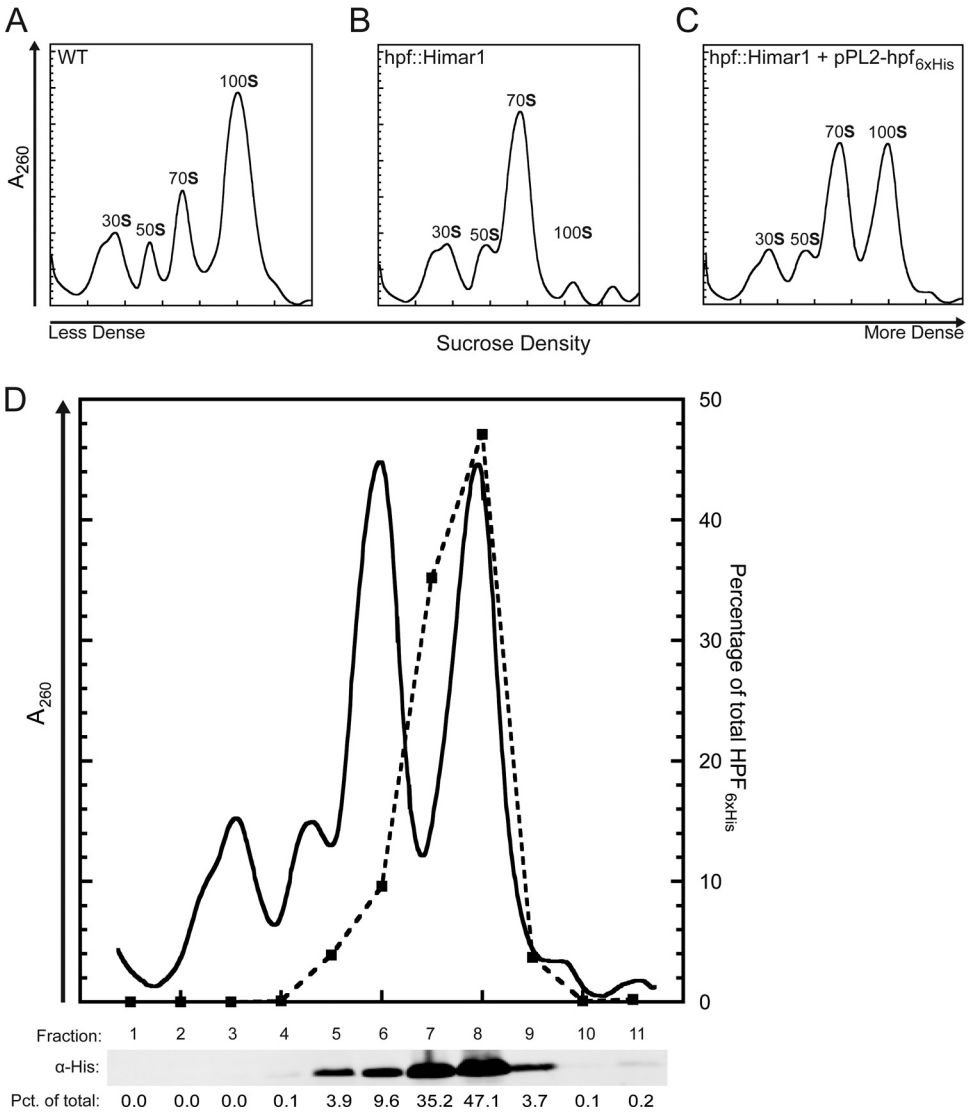

FIG 3 Role of HPF in 100S ribosome formation, and migration of HPF through sucrose density gradients. SDGC profiles of ribosomes collected from WT *L. monocytogenes* (A), *hpf*::*Himar1* mutant (B), and *hpf*::*Himar1* mutant complemented with pPL2-$hpf_{6\times His}$ (C) at the transition between logarithmic and stationary phase. (D) Western blot analysis of fractions collected from sucrose density gradients of *hpf*::*Himar1* mutant complemented with pPL2-$hpf_{6\times His}$. The plot shows A_{260} across sucrose gradient (solid line) and percentage of total $HPF_{6\times His}$ in each fraction (dashed line). Western blot and numerical percentages of total signal are shown below.

timing of this mRNA abundance profile resembled the profile of 100S ribosome formation shown above by SDGC (Fig. 2).

Based on previous work showing a correlation between hibernation and nutrient content of growth medium in *S. aureus* (9), we hypothesized that the presence of usable carbon sources might influence expression of *hpf* in *L. monocytogenes*. We exposed mid-log-phase bacteria to stationary-phase conditioned medium supplemented with glucose and measured transcript levels. This treatment reduced *hpf* expression to levels similar to those seen in fresh medium (Fig. 4B). The reduction in *hpf* expression was accompanied by a reduction in the ratio of 100S to 70S ribosomes (Fig. 4D). Based on these observations, it appears that a large proportion of *hpf* upregulation during the transition to stationary phase is mediated by carbon starvation.

Transcriptional control of the *hpf* gene by two alternative sigma factors, σ^B and σ^H, has been reported in *L. monocytogenes* and *B. subtilis* (30–32). Sigma B coordinates the transcription of genes required for the general stress response (33). To determine the stress responsiveness of *hpf* transcript abundance, we grew bacteria to mid-log phase and then exposed them to one of several stressful conditions for a period of 5 min. We found that 4% (vol/vol) ethanol, 4% (wt/vol) sodium chloride, and 46°C heat shock were all efficient inducers of *hpf* expression. Use of a *sigB*-deficient strain abrogated the upregulation of *hpf* observed in WT bacteria in response to all of these stresses (Fig. 4C), indicating that hibernation-mediated responses to these stresses was dependent upon σ^B.

HPF-deficient *L. monocytogenes* is similar to the WT in most *in vitro* fitness assays. We subjected the *hpf*::*Himar1* strain to a variety of *in vitro* assays commonly used to assess fitness and vir-

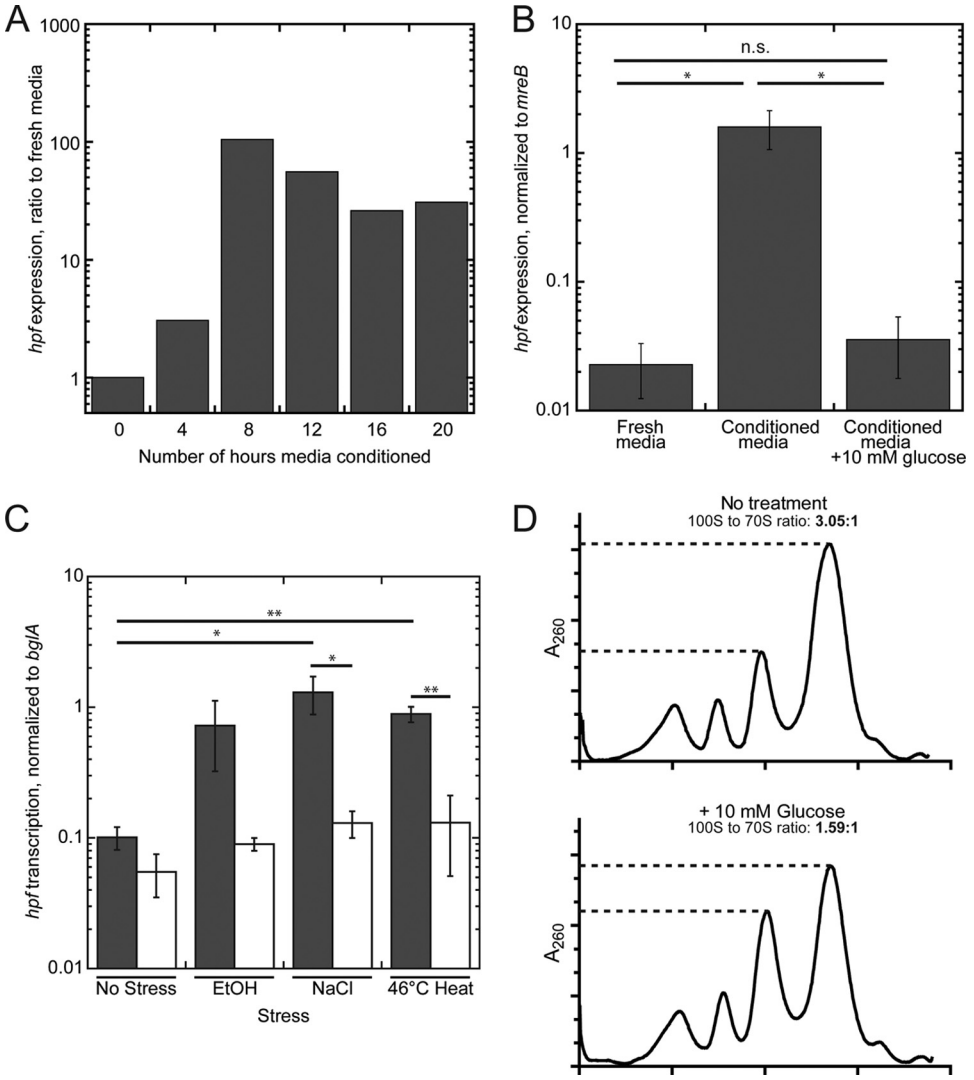

FIG 4 Transcriptional regulation of *hpf*. (A to C) Quantitative RT-PCR of *hpf* transcripts under various conditions. (A) *hpf* transcriptional response of WT *L. monocytogenes* grown to mid-log phase and then treated for 30 min with BHI conditioned by WT bacteria for various lengths of time. (B) *hpf* transcriptional response of WT *L. monocytogenes* grown to mid-log phase and treated with BHI conditioned for 8 h by WT bacteria, with and without added glucose as noted. (C) Stress-induced *hpf* transcription by mid-log WT (gray bars) and Δ*sigB* (white bars) bacteria treated for 5 min with unaltered BHI, BHI and 4% (vol/vol) ethanol, BHI and 4% (wt/vol) NaCl, or BHI at 46°C. (D) Sucrose density gradient profiles of bacteria treated with the listed conditions for 30 min prior to lysis and preparation of ribosomes. Ribosomal peak ratios were determined by integration of the area under each peak. *, $P < 0.05$; **, $P < 0.01$.

ulence of *L. monocytogenes*. Bacterial growth curves in rich medium showed that the *hpf*::*Himar1* strain had a slightly increased doubling time compared to that of the WT during exponential-phase growth (43 compared to 40 min). An intracellular survival and growth assay in resting bone marrow-derived macrophages showed only small differences between WT and *hpf* mutant bacteria (data not shown). Based on infection and growth kinetics in this assay, the *L. monocytogenes hpf*::*Himar1* strain appeared to invade, escape, and replicate very similarly to the WT. One method that is commonly used as a predictor of relative virulence in *L. monocytogenes* involves infecting a monolayer of mouse fibroblasts and observing the formation of plaques as bacteria invade, spread, and lyse host cells. This plaque assay revealed no significant defects for the *hpf*::*Himar1* strain, indicating that the mutant invades, grows, and spreads similarly to the WT (data not shown).

HPF mutant bacteria show a competitive survival disadvantage to the WT in rich medium. Since *hpf* expression is so highly induced by nutrient-depleted medium and in stressful conditions, and since the inability to hibernate reduces the fitness of several hibernation-deficient bacterial mutants during prolonged post-exponential-phase growth (7), we reasoned that an *L. monocytogenes hpf* mutant was most likely to display growth or survival defects when exposed to stationary-phase conditions. Surprisingly, the *hpf*::*Himar1* mutant survived similarly to the WT when each was grown in pure culture in rich medium over a period of 13 days (data not shown). However, when *hpf* transposon insertion mutants were grown in competitive coculture with WT bacteria, they displayed a striking defect in post-exponential-phase survival. After 4 days in competition with the WT, the *L. monocytogenes hpf*::*Himar1* strain comprised an average of only 1/100th of the total number of CFU, while *Himar1* insertion mutants selected

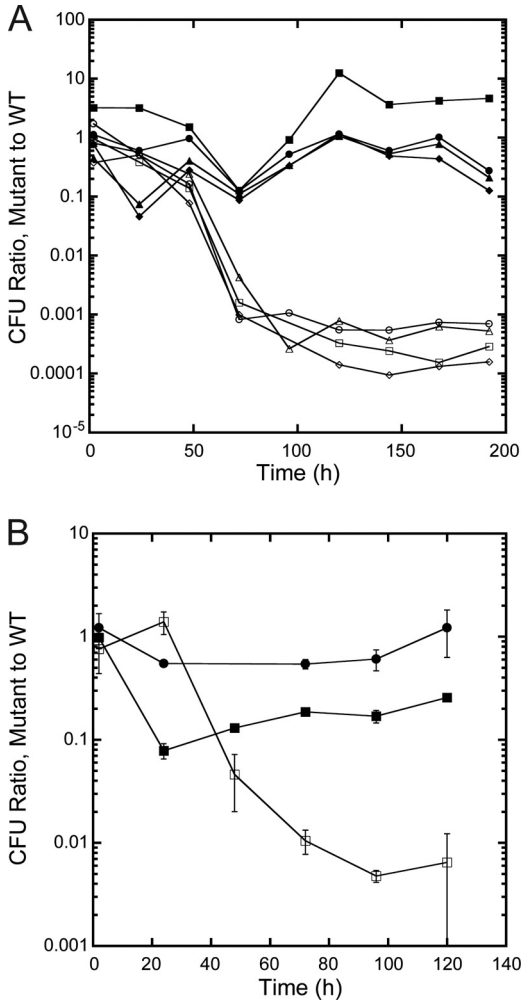

FIG 5 Competition experiments in rich medium. Strains indicated below were coinoculated at a 1:1 ratio into autoclave-sterilized BHI. Cultures were incubated at 37°C, and samples were diluted and plated for CFU every 24 h. (A) Randomly selected *Himar1* transposon insertion mutants (filled symbols) or the *hpf*::*Himar1* strain (open symbols) were each competed with WT in BHI. The data presented are from four separate competition experiments. (B) *hpf*::*Himar1* strain (open squares), *hpf*::*Himar1* strain with pPL2-hpf_{FLAG} (closed squares), and DP-L3903 (circles; control strain carrying an Erm^r transposon insertion at a separate site) were each competed with WT in BHI. Data shown represent one of several similar experiments performed in duplicate.

at random from a transposon insertion library maintained populations roughly equivalent to that of the WT over the same period (Fig. 5A). Although the magnitude varied, this survival defect appeared consistently. Complementation of the *hpf*::*Himar1* strain with pPL2-hpf_{FLAG} largely rescued the competitive defect (Fig. 5B).

HPF plays a role in survival in a mouse model of infection. Although HPF is conserved across a diverse array of bacteria (10), the role of ribosome hibernation in the virulence of a human pathogen remains untested. We used an intravenous mouse model of *L. monocytogenes* infection to determine whether *hpf*-deficient bacteria were less fit for growth and survival in association with a mammalian host. Groups of mice were infected in parallel with WT, Δ*hpf*, or complemented Δ*hpf* (Δ*hpf* with pPL2-*hpf*) bacteria via tail vein injection, and the number of CFU per organ was determined by plating 48 h postinfection. This procedure revealed a median of 6-fold-fewer CFU per organ in the spleens and 12-fold-fewer CFU per organ in the livers of Δ*hpf* mutant-infected mice than WT-infected mice, defects that were absent in mice infected with the complemented strain (Fig. 6A). Despite the importance and abundance of HPF in stationary phase, infection with stationary phase or 3-day-old WT or HPF-deficient bacteria produced no additional virulence defect (data not shown).

Because *L. monocytogenes* infection occurs primarily through ingestion of contaminated food, we also examined the oral route of infection to determine whether any of the stresses associated with traveling through the gastrointestinal tract would impact virulence of HPF-deficient bacteria. Like the intravenous infections, these oral infections showed defects in the livers (3-fold) and spleens (8-fold) of Δ*hpf*-infected animals compared to those in WT-infected animals (Fig. 6B).

DISCUSSION

Ribosome hibernation has been recognized as an adaptive behavior in bacteria for more than 20 years, but its precise role remains unclear. In this work, we found that HPF is essential for ribosome hibernation in *L. monocytogenes* and that *hpf*-deficient bacteria experience a disadvantage in competitive coculture. Our results also indicated that HPF is involved in the bacterial response to various stressful conditions and is important for optimal pathogenesis.

The presence of hibernating ribosomes in *L. monocytogenes* during exponential-phase growth closely resembled the hibernation profiles previously observed in *S. aureus* (9). In contrast, several studies have shown that *E. coli* produces almost no 100S ribosomes until the beginning of stationary phase (7, 8, 12). The presence of large numbers of 100S ribosomes during exponential-phase growth (Fig. 2) suggests that ribosome hibernation may serve an important function even during exponential-phase growth, an idea that is supported by the small growth defect seen in HPF-deficient *L. monocytogenes*. The surprising abundance of hibernating ribosomes in extracts from exponential-phase bacteria may also be an indicator of yet-unrecognized heterogeneity within *L. monocytogenes* monocultures. The approximate 1:1 ratio of 70S to 100S ribosomes during mid-log-phase growth (Fig. 2) may be derived from two distinct populations: one that is actively growing and contributes very few 100S ribosomes and another that is dormant and contributes the majority of the observed 100S ribosomes. Alternatively, hibernation may be tied to the bacterial replication cycle, temporarily reducing translation to ease partitioning of cellular components or shunting energy into the structural rearrangements associated with cell division. The reduction of translational output during cell division is a behavior that has been reported previously in eukaryotes (34). The presence of dormant subpopulations within bacterial cultures at various growth phases has been well documented. For example, persister cells have been observed within normal, exponentially growing populations of bacteria and are thought to be small nongrowing subpopulations that are more resistant to insults than actively growing cells (35). In addition, *L. monocytogenes* has previously been shown to adapt to long-term stationary phase (called growth advantage at stationary phase [GASP]) in a partially σ^B-dependent manner (36). The possibility that ribosome hibernation is con-

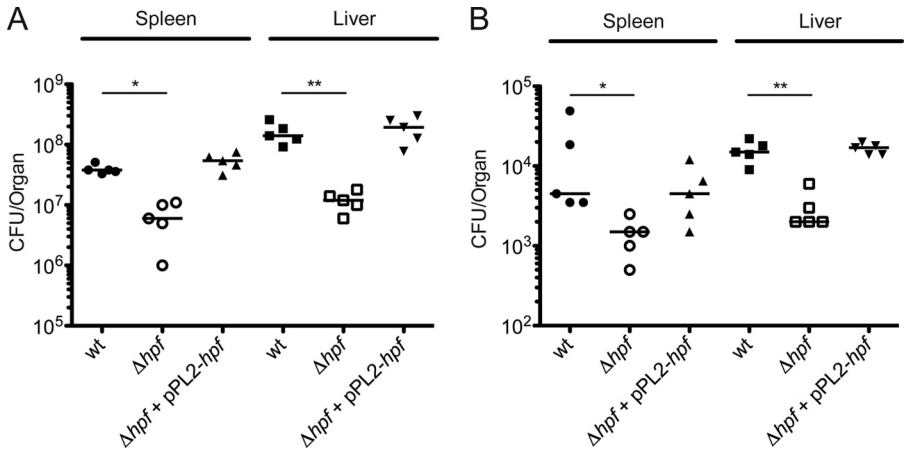

FIG 6 Intravenous and oral mouse infections. Total bacterial load was measured from the spleens and livers of BALB/c mice 48 h postinfection with *L. monocytogenes* WT strain, Δ*hpf* mutant, or Δ*hpf* mutant complemented with pPL2-*hpf*. (A) Intravenous infection with 3×10^4 bacteria. (B) Oral infection with 1×10^8 bacteria by ingestion on food. Significant differences are noted: *, $P < 0.05$; **, $P < 0.01$.

nected to the persister cell or GASP phenotypes in *L. monocytogenes* warrants further investigation.

Ueta et al. have speculated that the hibernation behavior of *S. aureus*, particularly the decrease in abundance of 100S ribosomes and the redistribution of *S. aureus* HPF into the 70S pool during post-exponential-phase growth, might correspond to the need for *S. aureus* cells to adhere to one another and begin expressing virulence factors (9). Interestingly, we originally identified the *hpf*::*Himar1* strain as a hyperhemolytic mutant, and the *L. monocytogenes* hemolysin, LLO, is preferentially translated during late logarithmic phase and stationary phase (37, 38). The mechanism underlying this regulation is unknown; it is possible that ribosome hibernation plays a role in modulating virulence factor expression in *L. monocytogenes* as well. The idea that more labile 70S-HPF complexes might be responsible for virulence gene expression is intriguing, and it is tempting to speculate that hibernation might serve as a mechanism for preferential translation of specific messages during times of need or stress. However, the lack of virulence defects in the *in vitro* assays argues against a significant role for HPF in virulence gene expression.

While *rmf* and *hpf* expression have been shown to increase at the transition between exponential phase and stationary phase in Gram-negative bacteria (12, 17), it was previously unknown what specific stimuli caused expression of *hpf* and induction of hibernation during broth growth of *L. monocytogenes*. We found that nutrient depletion triggers *hpf* induction during the transition from exponential to stationary phase since treatment of mid-log-phase bacteria with stationary-phase conditioned medium stimulated an approximately 100-fold increase in *hpf* mRNA abundance compared to that of fresh medium (Fig. 4A). Two primary changes in the growth medium might stimulate hibernation. First, it is possible that bacterial conditioning of the medium resulted in accumulation of a bacterial molecule that induced *hpf* expression. Alternatively, it is possible that bacterial growth depleted the medium of some nutrient essential for growth and that this depletion stimulated hibernation. Ueta et al. showed that the nutrient richness influenced the extent of ribosome dimerization by *S. aureus*, but they did not investigate what nutrients were responsible for induction of hibernation (9). We determined that the abundance of *hpf* transcript in conditioned growth medium was strongly responsive to glucose content. Supplementation of conditioned medium with glucose restored *hpf* transcript levels to roughly those seen in fresh medium (Fig. 4B) and produced a concomitant decrease in the ratio of 100S to 70S ribosomes (Fig. 4D). These observations indicate that carbon starvation stimulates ribosome hibernation, and it is possible that other nutritional signals act in a similar way.

In addition to nutrient availability, stressful conditions also appear to influence *hpf* regulation. We observed approximately 10-fold increases in *hpf* expression upon salt, ethanol, and heat stress, all of which were abrogated in the absence of the stress-responsive sigma factor σ^B (Fig. 4C). These observations are in agreement with the published data that σ^B and σ^H regulate *hpf* expression in *L. monocytogenes* and *B. subtilis* (30, 31) and reinforce the role for HPF in stress tolerance of Gram-positive bacteria. In contrast to these expression data, HPF has not appeared as a σ^B-regulated protein in published proteomic analyses of the σ^B regulon in response to various stresses in *L. monocytogenes* (39–41). This disconnect between *hpf* expression and protein abundance suggests that another layer of posttranscriptional *hpf* regulation may exist in Gram-positive bacteria.

Despite the striking changes in transcript abundance discussed above, physiological changes caused by HPF deficiency have proven somewhat elusive. One of the few physiological phenotypes observed thus far in hibernation-deficient bacteria is the survival defect displayed by RMF-deficient bacteria during growth in nutrient-poor conditions. *E. coli* Δ*rmf* mutants display wild-type (WT) viability in culture for approximately 2 days and then die rapidly and yield 1,000-fold fewer CFU after 5 days of incubation (7). Similarly, RMF-deficient *P. aeruginosa* in deep layers of biofilms displays substantially reduced survival (42), and HPF-deficient *L. lactis* displays reduced survival and recovery from starvation (14). Despite being unable to form 100S ribosomes (similar to an *E. coli* RMF mutant), *L. monocytogenes* HPF mutants survived post-exponential-phase growth in monoculture comparably to the WT. It was only in competitive coculture that HPF mutant *L. monocytogenes* showed a severe post-exponential-phase survival defect (Fig. 5). This competitive defect has the potential to be important for the success of *L. monocytogenes* as a pathogen. Because the majority of time spent in the environment is spent in

association with other bacterial populations, the ability to compete effectively for nutrients is critical for survival.

Determining how ribosome hibernation influences competitive survival will provide valuable insight into at least one of its cellular functions. Given HPF's extensive conservation, it is reasonable to speculate that ribosome hibernation plays other roles in addition to those examined above. If the hibernation machinery plays a general role in increasing bacterial fitness under certain stressful conditions, it may also prove to be a viable target for antimicrobials to combat a wide range of bacterial pathogens.

ACKNOWLEDGMENTS

We thank J. Leber for providing a valuable *hpf* transposon insertion mutant, A. Jackson and S. Covarrubias for help with sucrose density gradient centrifugation and the associated analysis, J. Zemansky for his work on the screen that led to these experiments, T. Burke for his work contributing to the Δ*hpf* mutant, and W. Hanson and A. Bitar for their generous gifts of pBHE261 and the Δ*sigB* deletion mutant, respectively.

This work was supported by the National Institutes of Health under Ruth L. Kirschstein National Research Service award F32 AI108253-01 (S.L.M.), Agriculture and Food Research Initiative competitive grant 2013-67012-21274 from the USDA National Institute of Food and Agriculture (S.L.M.), National Institutes of Health grant 1PO1 AI63302 (D.A.P.), and National Institutes of Health grant 1R01 AI27655 (D.A.P.).

Daniel A. Portnoy has a consulting relationship with and a financial interest in Aduro Biotech, and both he and the company stand to benefit from the commercialization of the results of this research.

REFERENCES

1. **Becavin C, Bouchier C, Lechat P, Archambaud C, Creno S, Gouin E, Wu Z, Kuhbacher A, Brisse S, Pucciarelli MG, Garcia-del Portillo F, Hain T, Portnoy DA, Chakraborty T, Lecuit M, Pizarro-Cerda J, Moszer I, Bierne H, Cossart P.** 2014. Comparison of widely used *Listeria monocytogenes* strains EGD, 10403S, and EGD-e highlights genomic variations underlying differences in pathogenicity. mBio 5(2):e00969–14. http://dx.doi.org/10.1128/mBio.00969-14.
2. **Vazquez-Boland JA, Kuhn M, Berche P, Chakraborty T, Dominguez-Bernal G, Goebel W, Gonzalez-Zorn B, Wehland J, Kreft J.** 2001. Listeria pathogenesis and molecular virulence determinants. Clin Microbiol Rev **14:**584–640. http://dx.doi.org/10.1128/CMR.14.3.584-640.2001.
3. **Gray MJ, Freitag NE, Boor KJ.** 2006. How the bacterial pathogen *Listeria monocytogenes* mediates the switch from environmental Dr. Jekyll to pathogenic Mr. Hyde. Infect Immun **74:**2505–2512. http://dx.doi.org/10.1128/IAI.74.5.2505-2512.2006.
4. **de las Heras A, Cain RJ, Bielecka MK, Vazquez-Boland JA.** 2011. Regulation of *Listeria* virulence: PrfA master and commander. Curr Opin Microbiol **14:**118–127. http://dx.doi.org/10.1016/j.mib.2011.01.005.
5. **Kato T, Yoshida H, Miyata T, Maki Y, Wada A, Namba K.** 2010. Structure of the 100S ribosome in the hibernation stage revealed by electron cryomicroscopy. Structure **18:**719–724. http://dx.doi.org/10.1016/j.str.2010.02.017.
6. **Wada A, Igarashi K, Yoshimura S, Aimoto S, Ishihama A.** 1995. Ribosome modulation factor: stationary growth phase-specific inhibitor of ribosome functions from *Escherichia coli*. Biochem Biophys Res Commun **214:**410–417. http://dx.doi.org/10.1006/bbrc.1995.2302.
7. **Yamagishi M, Matsushima H, Wada A, Sakagami M, Fujita N, Ishihama A.** 1993. Regulation of the *Escherichia coli rmf* gene encoding the ribosome modulation factor: growth phase- and growth rate-dependent control. EMBO J **12:**625–630.
8. **Wada A, Mikkola R, Kurland CG, Ishihama A.** 2000. Growth phase-coupled changes of the ribosome profile in natural isolates and laboratory strains of *Escherichia coli*. J Bacteriol **182:**2893–2899. http://dx.doi.org/10.1128/JB.182.10.2893-2899.2000.
9. **Ueta M, Wada C, Wada A.** 2010. Formation of 100S ribosomes in *Staphylococcus aureus* by the hibernation promoting factor homolog SaHPF. Genes Cells **15:**43–58. http://dx.doi.org/10.1111/j.1365-2443.2009.01364.x.
10. **Ueta M, Ohniwa RL, Yoshida H, Maki Y, Wada C, Wada A.** 2008. Role of HPF (hibernation promoting factor) in translational activity in *Escherichia coli*. J Biochem **143:**425–433. http://dx.doi.org/10.1093/jb/mvm243.
11. **Ueta M, Yoshida H, Wada C, Baba T, Mori H, Wada A.** 2005. Ribosome binding proteins YhbH and YfiA have opposite functions during 100S formation in the stationary phase of *Escherichia coli*. Genes Cells **10:**1103–1112. http://dx.doi.org/10.1111/j.1365-2443.2005.00903.x.
12. **Wada A, Yamazaki Y, Fujita N, Ishihama A.** 1990. Structure and probable genetic location of a "ribosome modulation factor" associated with 100S ribosomes in stationary-phase *Escherichia coli* cells. Proc Natl Acad Sci U S A **87:**2657–2661. http://dx.doi.org/10.1073/pnas.87.7.2657.
13. **Ueta M, Wada C, Daifuku T, Sako Y, Bessho Y, Kitamura A, Ohniwa RL, Morikawa K, Yoshida H, Kato T, Miyata T, Namba K, Wada A.** 2013. Conservation of two distinct types of 100S ribosome in bacteria. Genes Cells **18:**554–574. http://dx.doi.org/10.1111/gtc.12057.
14. **Puri P, Eckhardt TH, Franken LE, Fusetti F, Stuart MC, Boekema EJ, Kuipers OP, Kok J, Poolman B.** 2014. *Lactococcus lactis* YfiA is necessary and sufficient for ribosome dimerization. Mol Microbiol **91:**394–407. http://dx.doi.org/10.1111/mmi.12468.
15. **Wada A.** 1998. Growth phase coupled modulation of *Escherichia coli* ribosomes. Genes Cells **3:**203–208. http://dx.doi.org/10.1046/j.1365-2443.1998.00187.x.
16. **Tagami K, Nanamiya H, Kazo Y, Maehashi M, Suzuki S, Namba E, Hoshiya M, Hanai R, Tozawa Y, Morimoto T, Ogasawara N, Kageyama Y, Ara K, Ozaki K, Yoshida M, Kuroiwa H, Kuroiwa T, Ohashi Y, Kawamura F.** 2012. Expression of a small (p) ppGpp synthetase, YwaC, in the (p) ppGpp0 mutant of *Bacillus subtilis* triggers YvyD-dependent dimerization of ribosome. Microbiologyopen **1:**115–134. http://dx.doi.org/10.1002/mbo3.16.
17. **Maki Y, Yoshida H, Wada A.** 2000. Two proteins, YfiA and YhbH, associated with resting ribosomes in stationary phase *Escherichia coli*. Genes Cells **5:**965–974. http://dx.doi.org/10.1046/j.1365-2443.2000.00389.x.
18. **Williamson KS, Richards LA, Perez-Osorio AC, Pitts B, McInnerney K, Stewart PS, Franklin MJ.** 2012. Heterogeneity in *Pseudomonas aeruginosa* biofilms includes expression of ribosome hibernation factors in the antibiotic-tolerant subpopulation and hypoxia-induced stress response in the metabolically active population. J Bacteriol **194:**2062–2073. http://dx.doi.org/10.1128/JB.00022-12.
19. **El-Sharoud WM, Niven GW.** 2007. The influence of ribosome modulation factor on the survival of stationary-phase *Escherichia coli* during acid stress. Microbiology **153:**247–253. http://dx.doi.org/10.1099/mic.0.2006/001552-0.
20. **Garay-Arroyo A, Colmenero-Flores JM, Garciarrubio A, Covarrubias AA.** 2000. Highly hydrophilic proteins in prokaryotes and eukaryotes are common during conditions of water deficit. J Biol Chem **275:**5668–5674. http://dx.doi.org/10.1074/jbc.275.8.5668.
21. **Niven GW.** 2004. Ribosome modulation factor protects *Escherichia coli* during heat stress, but this may not be dependent on ribosome dimerisation. Arch Microbiol **182:**60–66. http://dx.doi.org/10.1007/s00203-004-0698-9.
22. **Crimmins GT, Schelle MW, Herskovits AA, Ni PP, Kline BC, Meyer-Morse N, Iavarone AT, Portnoy DA.** 2009. *Listeria monocytogenes* 6-phosphogluconolactonase mutants induce increased activation of a host cytosolic surveillance pathway. Infect Immun **77:**3014–3022. http://dx.doi.org/10.1128/IAI.01511-08.
23. **Camilli A, Tilney LG, Portnoy DA.** 1993. Dual roles of *plcA* in *Listeria monocytogenes* pathogenesis. Mol Microbiol **8:**143–157. http://dx.doi.org/10.1111/j.1365-2958.1993.tb01211.x.
24. **Horton RM, Hunt HD, Ho SN, Pullen JK, Pease LR.** 1989. Engineering hybrid genes without the use of restriction enzymes: gene splicing by overlap extension. Gene **77:**61–68. http://dx.doi.org/10.1016/0378-1119(89)90359-4.
25. **Lauer P, Hanson B, Lemmens EE, Liu W, Luckett WS, Leong ML, Allen HE, Skoble J, Bahjat KS, Freitag NE, Brockstedt DG, Dubensky TW, Jr.** 2008. Constitutive activation of the PrfA regulon enhances the potency of vaccines based on live-attenuated and killed but metabolically active *Listeria monocytogenes* strains. Infect Immun **76:**3742–3753. http://dx.doi.org/10.1128/IAI.00390-08.
26. **Bou Ghanem EN, Jones GS, Myers-Morales T, Patil PD, Hidayatullah AN, D'Orazio SE.** 2012. InlA promotes dissemination of *Listeria monocytogenes* to the mesenteric lymph nodes during food borne infection of mice. PLoS Pathog 8:e1003015. http://dx.doi.org/10.1371/journal.ppat.1003015.
27. **Toledo-Arana A, Dussurget O, Nikitas G, Sesto N, Guet-Revillet H,**

Balestrino D, Loh E, Gripenland J, Tiensuu T, Vaitkevicius K, Barthelemy M, Vergassola M, Nahori MA, Soubigou G, Regnault B, Coppee J Y, Lecuit M, Johansson J, Cossart P. 2009. The *Listeria* transcriptional landscape from saprophytism to virulence. Nature **459:**950–956. http://dx.doi.org/10.1038/nature08080.

28. **Lauer P, Chow MY, Loessner MJ, Portnoy DA, Calendar R.** 2002. Construction, characterization, and use of two *Listeria monocytogenes* site-specific phage integration vectors. J Bacteriol **184:**4177–4186. http://dx.doi.org/10.1128/JB.184.15.4177-4186.2002.
29. **Okada Y, Makino S, Tobe T, Okada N, Yamazaki S.** 2002. Cloning of rel from *Listeria monocytogenes* as an osmotolerance involvement gene. Appl Environ Microbiol **68:**1541–1547. http://dx.doi.org/10.1128/AEM.68.4.1541-1547.2002.
30. **Chaturongakul S, Raengpradub S, Palmer ME, Bergholz TM, Orsi RH, Hu Y, Ollinger J, Wiedmann M, Boor KJ.** 2011. Transcriptomic and phenotypic analyses identify coregulated, overlapping regulons among PrfA, CtsR, HrcA, and the alternative sigma factors sigmaB, sigmaC, sigmaH, and sigmaL in *Listeria monocytogenes*. Appl Environ Microbiol **77:**187–200. http://dx.doi.org/10.1128/AEM.00952-10.
31. **Drzewiecki K, Eymann C, Mittenhuber G, Hecker M.** 1998. The *yvyD* gene of *Bacillus subtilis* is under dual control of sigmaB and sigmaH. J Bacteriol **180:**6674–6680.
32. **Eymann C, Hecker M.** 2001. Induction of sigma(B)-dependent general stress genes by amino acid starvation in a spo0H mutant of *Bacillus subtilis*. FEMS Microbiol Lett **199:**221–227. http://dx.doi.org/10.1111/j.1574-6968.2001.tb10678.x.
33. **O'Byrne CP, Karatzas KA.** 2008. The role of sigma B (sigma B) in the stress adaptations of *Listeria monocytogenes*: overlaps between stress adaptation and virulence. Adv Appl Microbiol **65:**115–140. http://dx.doi.org/10.1016/S0065-2164(08)00605-9.
34. **Sivan G, Kedersha N, Elroy-Stein O.** 2007. Ribosomal slowdown mediates translational arrest during cellular division. Mol Cell Biol **27:**6639–6646. http://dx.doi.org/10.1128/MCB.00798-07.
35. **Lewis K.** 2010. Persister cells. Annu Rev Microbiol **64:**357–372. http://dx.doi.org/10.1146/annurev.micro.112408.134306.
36. **Bruno JC, Jr, Freitag NE.** 2011. *Listeria monocytogenes* adapts to long-term stationary phase survival without compromising bacterial virulence. FEMS Microbiol Lett **323:**171–179. http://dx.doi.org/10.1111/j.1574-6968.2011.02373.x.
37. **Folio P, Chavant P, Chafsey I, Belkorchia A, Chambon C, Hebraud M.** 2004. Two-dimensional electrophoresis database of *Listeria monocytogenes* EGDe proteome and proteomic analysis of mid-log and stationary growth phase cells. Proteomics **4:**3187–3201. http://dx.doi.org/10.1002/pmic.200300841.
38. **Schnupf P, Portnoy DA.** 2007. Listeriolysin O: a phagosome-specific lysin. Microbes Infect **9:**1176–1187. http://dx.doi.org/10.1016/j.micinf.2007.05.005.
39. **Abram F, Starr E, Karatzas KA, Matlawska-Wasowska K, Boyd A, Wiedmann M, Boor KJ, Connally D, O'Byrne CP.** 2008. Identification of components of the sigma B regulon in *Listeria monocytogenes* that contribute to acid and salt tolerance. Appl Environ Microbiol **74:**6848–6858. http://dx.doi.org/10.1128/AEM.00442-08.
40. **Abram F, Su WL, Wiedmann M, Boor KJ, Coote P, Botting C, Karatzas KA, O'Byrne CP.** 2008. Proteomic analyses of a *Listeria monocytogenes* mutant lacking sigmaB identify new components of the sigmaB regulon and highlight a role for sigmaB in the utilization of glycerol. Appl Environ Microbiol **74:**594–604. http://dx.doi.org/10.1128/AEM.01921-07.
41. **Shin JH, Kim J, Kim SM, Kim S, Lee J C, Ahn J M, Cho JY.** 2010. sigmaB-dependent protein induction in *Listeria monocytogenes* during vancomycin stress. FEMS Microbiol Lett **308:**94–100. http://dx.doi.org/10.1111/j.1574-6968.2010.01998.x.
42. **Williamson KS, Richards LA, Perez-Osorio AC, Pitts B, McInnerney K, Stewart PS, Franklin MJ.** 17 February 2012. Heterogeneity in *Pseudomonas aeruginosa* biofilms includes expression of ribosome hibernation factors in the antibiotic tolerant subpopulation and hypoxia induced stress response in the metabolically active population. J Bacteriol http://dx.doi.org/10.1128/JB.00022-12.
43. **Goujon M, McWilliam H, Li W, Valentin F, Squizzato S, Paern J, Lopez R.** 2010. A new bioinformatics analysis tools framework at EMBL-EBI. Nucleic Acids Res **38:**W695–W699. http://dx.doi.org/10.1093/nar/gkq313.
44. **Larkin MA, Blackshields G, Brown NP, Chenna R, McGettigan PA, McWilliam H, Valentin F, Wallace IM, Wilm A, Lopez R, Thompson J D, Gibson TJ, Higgins DG.** 2007. Clustal W and Clustal X version 2.0. Bioinformatics **23:**2947–2948. http://dx.doi.org/10.1093/bioinformatics/btm404.
45. **Waterhouse AM, Procter JB, Martin DM, Clamp M, Barton GJ.** 2009. Jalview version 2—a multiple sequence alignment editor and analysis workbench. Bioinformatics **25:**1189–1191. http://dx.doi.org/10.1093/bioinformatics/btp033.
46. **Vila-Sanjurjo A, Schuwirth BS, Hau CW, Cate JH.** 2004. Structural basis for the control of translation initiation during stress. Nat Struct Mol Biol **11:**1054–1059. http://dx.doi.org/10.1038/nsmb850.
47. Reference deleted.
48. **Bishop DK, Hinrichs DJ.** 1987. Adoptive transfer of immunity to *Listeria monocytogenes*. The influence of *in vitro* stimulation on lymphocyte subset requirements. J Immunol **139:**2005–2009.
49. **Auerbuch V, Lenz LL, Portnoy DA.** 2001. Development of a competitive index assay to evaluate the virulence of *Listeria monocytogenes actA* mutants during primary and secondary infection of mice. Infect Immun **69:**5953–5957. http://dx.doi.org/10.1128/IAI.69.9.5953-5957.2001.
50. **Smith K, Youngman P.** 1992. Use of a new integrational vector to investigate compartment-specific expression of the *Bacillus subtilis spoIIM* gene. Biochimie **74:**705–711. http://dx.doi.org/10.1016/0300-9084(92)90143-3.